ACS APPLIED MATERIALS & INTERFACES

Research Article

www.acsami.org

Electrohydrodynamic Jet-Printed Zinc–Tin Oxide TFTs and Their Bias Stability

Yong Gu Lee and Woon-Seop Choi*

Department of Display Engineering, Hoseo University, Asan-city, Chungnam 336-795, Korea

Supporting Information

ABSTRACT: Zinc–tin oxide (ZTO) thin-film transistors (TFTs) were fabricated using an electrohydrodynamic-jet (EHD-jet) printing technique at annealing temperatures ranging from 300 to 500 °C. An EHD-jet-printed ZTO active layer was patterned with a 60 μm width using a 100 μm inner diameter metal nozzle. The electrical properties of an EHD-jet-printed ZTO TFT showed a mobility of 9.82 $cm^2/(V\ s)$, an on–off current ratio of 3.7×10^6, a threshold voltage of 2.36 V, and a subthreshold slope of 0.73 V/dec at 500 °C. Significantly improved properties were obtained compared to the spin-coated and inkjet-printed ones. Better hysteresis behavior and positive bias stability of the ZTO TFTs were also achieved using EHD-jet printing technology.

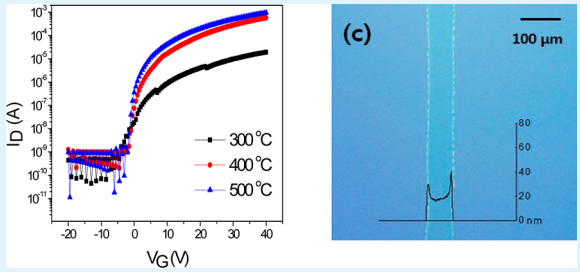

KEYWORDS: *electrohydrodynamic-jet, EHD-jet, oxide TFTs, ZTO, printing, bias stability*

INTRODUCTION

Since active-matrix organic light-emitting diodes and active-matrix liquid crystal displays have been commercialized, there has been increasing demand for next-generation displays with high resolution, rapid response time, simple process and large-area manufacturing with low cost.[1] The key to meet this demand is the thin-film transistor (TFT) backplane technology for displays. Amorphous Si (a-Si) TFTs and poly Si TFTs as backplanes are unsuitable for such purposes because of the low mobility of a-Si TFT and the laser process of poly Si TFT. In addition, OTFTs (organic TFTs) have low electron/hole mobility and short lifetimes.[2]

Oxide TFTs have advantages, such as higher field effect mobility than a-Si TFT, lower cost process than poly Si, and eco-friendly, and can be applied to large area and solution methods. For this reason, oxide TFTs have attracted attention as a potential candidate for the backplane of next-generation displays. Another reason is that zinc-based oxide TFTs show high mobility and a wide band gap, making them transparent. Most oxide TFTs are fabricated using vacuum techniques, such as atomic-layer deposition, DC or radio frequency sputtering, and ion-beam deposition.[3,4] Vacuum processes have disadvantages in that they are not suitable for large-area deposition and are expensive. Solution processes are simpler and more eco-friendly than vacuum processes, and the representative solution processes are spin coating, inkjet printing, screen printing, gravure printing, and electrohydrodynamic jet (EHD-jet) printing. Solution process using metal salt or metal alkoxide precursor is a widely known solution deposition technique that provides not only easy and low-cost preparation of a large-area thin film, but also easy control over the film composition and thickness uniformity.[5] Spin coating requires an additional patterning process for selective deposition and also wastes a large fraction of the material.[6] On the other hand, inkjet printing and EHD-jet printing are used as a drop-on-demand printing process for noncontact printing without a complex photolithography process.[6] Inkjet printing is operated by the principle of a piezoelectric field and obtains the desired patterning by changing the waveform. EHD-jet printing can provide simple patterning and complex patterning with better resolution. The process can use an electric field to create jetting droplets for the delivery of a liquid portion to a designated substrate.[7] Although inkjet printing is greatly influenced by the ink viscosity, EHD-jet printing can produce any pattern with a charged ink formulation with less viscosity dependence. Many types of oxide TFTs, for example, zinc–tin oxide (ZTO), indium oxide (In_2O_3), indium-gallium-zinc oxide (IGZO), etc., have been fabricated by solution processes. Among them, ZTO has attracted considerable attention as an indium–free and inexpensive zinc material.

Indium–zinc oxide (IZO) TFTs fabricated from EHD-jet printing was reported to have a very high resolution using a 2 μm glass needle coated with Au/Pd and hydrophobic surface treatment, which is expensive and not practical, to obtain <20 μm channel width, but it showed relatively low mobility of 3.7 $cm^2/(V\ s)$.[8] Very recently, IGZO TFTs were reported by solution-process and EHD-jet process.[9] They used a 10 μm glass needle coated with the same metallic coating and surface treatment to obtain a relatively low mobility of 1.3 $cm^2/(V\ s)$ with 30 μm channel width. Nevertheless the TFT properties using EHD-jet have not been investigated systematically. ZTO TFTs have been fabricated using an EHD spray technique.[10]

Received: February 18, 2014
Accepted: July 7, 2014
Published: July 7, 2014

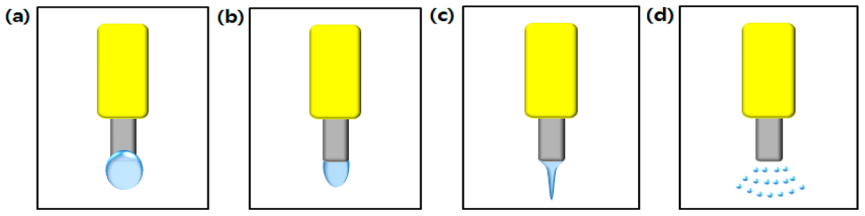

Figure 1. Schematic jetting profiles of electrohydrodynamic-jet printer with jetting voltages of (a) 0 kV, (b) 2 kV, (c) 2.5 kV, and (d) 3.5 kV.

In this study, ZTO TFTs were fabricated by an EHD-jet printing process. A uniform active layer was obtained using a steel needle with an inner diameter of 100 μm without any treatments, a robust and simple process, to obtain a reasonable channel width and better mobility. Compared to the spin-coating process, ZTO TFTs using an EHD-jet process showed considerably improved electrical properties, indicating it to be a better processing technique.

EXPERIMENTAL SECTION

Bottom-gate and top-contact ZTO TFTs were fabricated using an EHD-jet printing process, which is similar to a previous report.[10] The 0.3 M ZTO solution precursor for the TFT devices was prepared by dissolving the same molar amount of zinc acetate ($Zn(CH_3COO)_2$) and tin chloride ($SnCl_2$) in 2-methoxyethanol with acetylacetone ($CH_3COCH_2COCH_3$) as the stabilizer and stirring the solution for 6 h at room temperature. The processing conditions for the EHD-jet were a jetting speed of 8000 μm/s and a substrate temperature of 50 °C. A steel nozzle tip (EFD-Korea) with an inner diameter of 100 μm for EHD-jet was used instead of the expensive and brittle glass capillary nozzle. The voltages between the substrate and nozzle tip were varied from 0 kV to 3.5 kV to obtain cone-type jetting. The ZTO active layers were deposited by the EHD-jet on a 300 nm thick SiO_2 gate insulator on a heavily doped silicon wafer being used as a gate electrode. The fabricated ZTO TFT device was annealed at temperatures ranging from from 300 to 500 °C for 1 h in air. A 100 nm electrode of aluminum as a source and drain electrode was deposited by thermal evaporation with a shadow mask to obtain a channel width of 750 μm and a channel length of 50 μm. All current–voltage (I–V) characterizations were measured using a semiconductor parameter analyzer (Keithly 4200) in a dark room at room temperature. The bias stability was measured under a gate voltage of 20 V with a gate bias stress for 1800 s. The thickness of the ZTO thin film was measured using a surface profilometer (Alpha Step 200, Tencor). The crystallinity of the thin film was analyzed by X-ray diffraction (XRD). The contact angle was measured using a DSA100. The surface topology was examined by atomic force microscopy (AFM, Park System, SE-70) in noncontact mode. X-ray photoelectron spectroscopy (XPS, Thermo VG ESCA Sigma Probe) was performed at 15 kV and 100 W using a monochromatic Al Kα radiation source. The surface was cleaned by Ar^+ etching (2 kV, 1.8 μA), and the spectra were calibrated using the C 1s peak.

RESULTS AND DISCUSSION

In the EHD-jet printing system, the fluid is electrified and ejected through the nozzle with the assistance of an electrical force by applying a high voltage.[11] The nozzle tip and jetting formation from the nozzle with the applied voltages were observed as the liquid was ejected under a constant hydraulic pressure from the EHD jet. A metal needle tip with an inner diameter of 100 μm was used for EHD-jet printing. Previous studies used a 2 and 10 μm glass capillary needle with additional metal deposition and surface treatment.[8,9] Our metal tip is more suitable for a simple and robust process with low cost. After screening experiment to obtain proper EHD-jetting and Taylor cone for a ZTO precursor solution, ink formulation and jetting distance were predetermined as approximately 0.3 M and 500 μm, respectively. The jetting voltage was controlled to obtain a proper cone-jet and draw the line pattern on the substrate, as shown in Figure 1. In the case of 0 kV, the voltage does not apply to the tip. A liquid droplet reached the end of tip due to the repulsive pressure from the syringe. At the same time, the liquid droplet formed and stood on the nozzle due to the higher surface tension of the liquid than the gravity applied to the liquid. When a bias voltage is applied to the nozzle tip, an electric field can be formed between the liquid and substrate, resulting in a narrow jetting from the nozzle tip. When the applied voltage is more than 2.5 kV, the electric force overcomes the gravity force, and the jetting shape becomes a cone-jet type for printing. Over 2.5 kV, the electric force is too large for jetting the liquid, and the liquid droplet transforms to a spray-type as reported previously.[10]

Before EHD-jet printing, a UV/O_3 treatment was conducted on the surface of SiO_2 to remove any organic residuals and improve the wetting property. To examine the wetting properties depending on the surface treatment, the contact angles were measured using a droplet of DI water on the wafer with and without the UV/O_3 treatment. The results were a 61.5° contact angle without the UV/O_3 treatment and a 34.1° contact angle with the treatment (Figure S1 in the Supporting Information). The wetting attribute of the coating was improved by the UV/O_3 treatment. After the UV/O_3 treatment, EHD-jet printing using a ZTO solution confirmed that the printed line was coated with better film uniformity except coffee ring as shown in Figure 2. The surface profile of

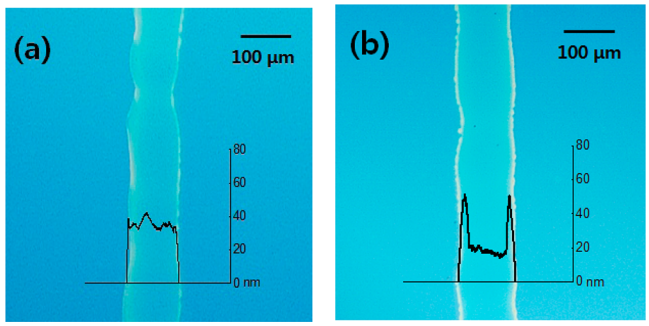

Figure 2. Optical microscopy images of EHD-jetted ZTO active pattern and their film profiles measured by profilometer (a) without UV/O_3 treatment and (b) with UV/O_3 treatment.

ZTO thin films on the untreated substrate showed a thicker film thickness with uneven surface roughness. This means that the wettability and pattern uniformity of the ZTO ink formulation on the SiO_2 was improved by the UV/O_3 treatment.

To realize high-resolution displays, it is important to produce TFTs with good characteristics, but it is also important to make narrow-patterned devices. Therefore, to obtain a narrow-

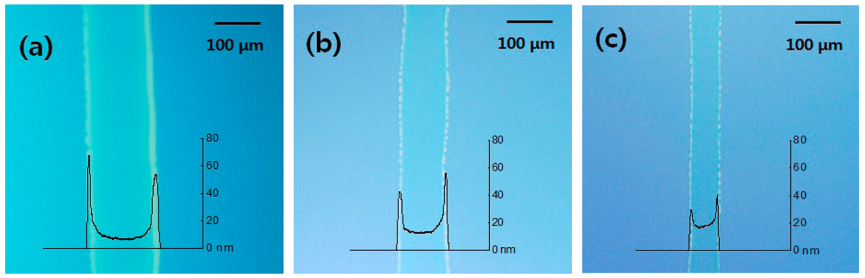

Figure 3. Optical microscopy images of EHD-jetted ZTO active pattern and their film profiles measured by profilometer with substrate moving rates of (a) 2000 μm/s, (b) 5000 μm/s, and (c) 8000 μm/s.

patterned ZTO active layer, two parameters need to be considered after determining jetting voltage, namely, the substrate temperature and the patterning speed of the EHD-jet equipment while active layers are formed. Average line widths of 130, 100, and 60 μm were obtained with the temperatures of 25, 50, and 75 °C, respectively, under a fixed substrate speed of 5000 μm/s. The EHD-jet showed the variation of the line width according to the substrate temperature. A narrow line width was obtained because ink jetting and solvent evaporation occur at the same time under high temperature. When the substrate temperature was 25 °C, the solvent still remained on the active layer that was formed during printing. When the substrate temperature was 75 °C, the printed line showed a different shape at the edge because the outside of the line showed more solvent evaporation than at 50 and 25 °C. This is similar to the coffee ring effect of the inkjet printing process.[12,13] Because the substrate temperature influences the diffusion and evaporation of the liquid droplet during jetting, the substrate temperature affects the line width and the characteristics of the TFTs. Therefore, more experiments were performed with the substrate speed at a fixed substrate temperature of 50 °C. The most affecting factor on the line width was the substrate moving speed on the stage. The average line widths were 150, 100, and 60 μm at the stage moving speed of 2000, 5000, and 8000 μm/s, respectively, as shown in Figure 3. As expected, a high-moving speed produced a lower contact time of the jetting precursor, and smaller amounts remained on the substrate, resulting in a respective thickness variation of 10, 15, and 20 nm.

To make a ZTO thin film for analysis, multiple EHD-jettings were performed on a designated area to make a relatively large size film. The XRD pattern did not show a peak at 34° 2 θ because of the amorphous states of ZTO thin films at various annealing times (Figure 4) as reported elsewhere.[14] However, a very small new cubic (3 2 2) peak was observed near 44.9° 2 θ in the ZTO thin film. The lattice constant for these peaks, which was calculated by Powder-X software, was a = 0.831 nm, which is close to that of the cubic Zn_2SnO_4 (a = 0.865 nm, JCPDS file 24−1470). These new peaks might be due to the formation of compounds, such as $(ZnO)_{1-x}(SnO_2)_x$, $(Zn_2SnO_4)_{1-x}(ZnO)_x$ and $(ZnSnO_3)_{1-x}(SnO_2)_x$, etc. as reported previously.[15] Figure 5 shows the result of XPS analysis of the O 1s core−shell for the ZTO thin films fabricated at 400 and 500 °C. The first low binding peak located at approximately 530 eV was related to O^{2-} ions associated with neighboring zinc and tin atoms (O_M), the second peak of approximately 531 eV was assigned to O^{2-} ions located in an oxygen-deficient region (O_{VAC}), and the third peak of 533 eV was related to the loosely bonded oxygen with water and OH groups on the surface (O_{OH}).[16] The O 1s peak indicated that

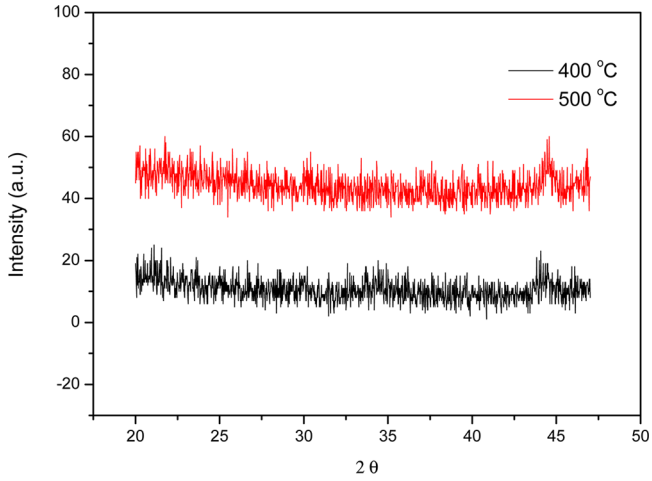

Figure 4. XRD spectra of EHD-jet printed ZTO thin films with annealing temperatures.

the $O_M/(O_M + O_{VAC} + O_{OH})$ value of the ZTO thin film fabricated at 500 °C was 64.68% larger than that of the ZTO thin film fabricated at 400 °C (63.57%) as shown in Table S1 in the Supporting Information. Zinc and tin components were confirmed at the Zn $2p_{3/2}$ (1021.5 eV) and Sn $3d_{5/2}$ (486.2 eV) peak in Table S1 in the Supporting Information and showed metal contents of 37.19% and 41.26% for 400 and 500 °C, respectively. The M−O bonding and M−M bonding strength increase with increasing processing temperature, resulting in improved mobility. An organic component, such as carbon, was removed during baking and annealing and was not observed by XPS (data not shown).

The electrical properties of the EHD-jet printed ZTO TFTs were compared with those of the spin-coated ones with 50 nm channel thickness (Table 1). The mobility of 9.82 $cm^2/(V\ s)$ for the EHD-jet ZTO TFTs was almost 3 times higher than that of the spin-coated TFTs. The mobility was higher than the mobility of 2.60−4.98 $cm^2/(V\ s)$ in the inkjet-printed ZTO TFTs.[17,18] There are multiple factors that influence mobility such as process parameter, ink formulation, gate dielectric selection, device geometry, etc. Even though much higher mobilities have been demonstrated in the literature[19,20] for solution-processed ZTO TFTs using a high-k dielectric and chlorine-based precursors, chloride precursors are not suitable for our system due to corrosive effect on metal needle. In the case of the EHD-spray ZTO TFTs, the mobility was 4.89 $cm^2/(V\ s)$, and the threshold voltage was 7.17 V.[10] A comparison of these printing methods reveals EHD-jet printing to have superior mobility and lower threshold voltage for operation. The electrical properties of the EHD-jet ZTO TFTs at 400 and

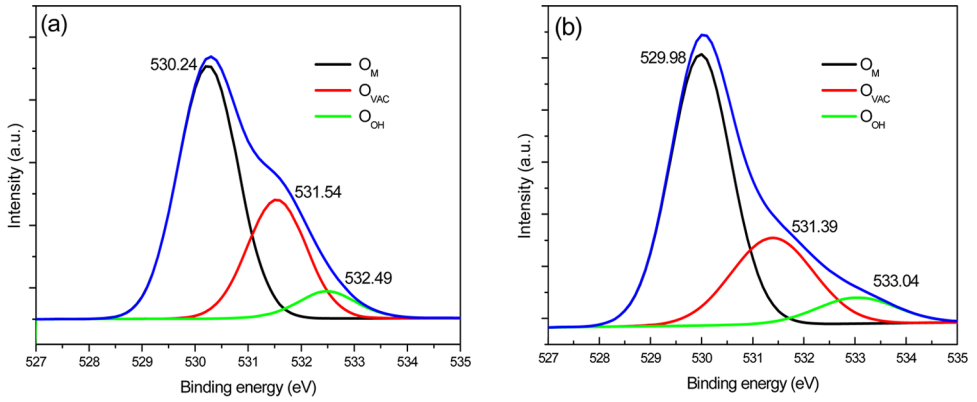

Figure 5. XPS spectra of the O 1s core−shell of EHD-jet printed ZTO thin films at (a) 400 °C and (b) 500 °C.

Table 1. Electric Properties of EHD-Jet Printed ZTO TFTs at Annealing Temperatures of 300, 400, and 500 °C

		TFT properties			
ZTO temp, °C	deposited method	mobility ($cm^2 V^{-1}s^{-1}$)	on/off ratio	V_{th} (V)	S−S (V dec^{-1})
300	spin coating				
400	spin coating	1.20	1.16×10^5	−0.31	2.71
500	spin coating	3.75	9.70×10^5	−2.09	0.50
300	EHD-jet	0.23	2.76×10^5	3.33	1.81
400	EHD-jet	7.99	1.93×10^6	4.91	0.82
500	EHD-jet	9.82	3.68×10^6	2.16	0.73

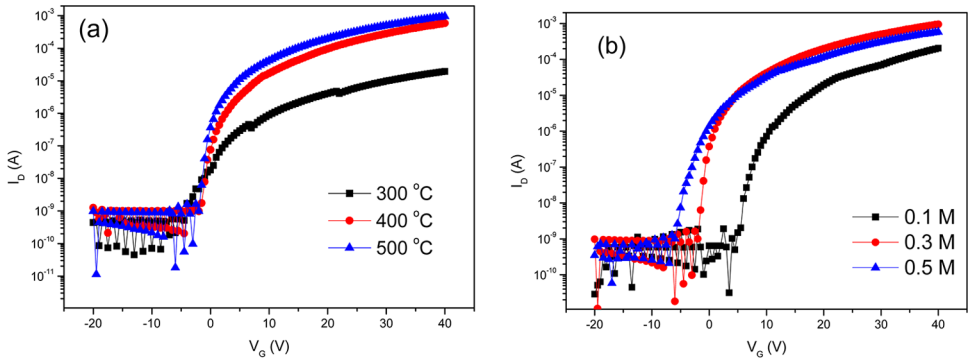

Figure 6. Transfer characteristics of the EHD-jet printed ZTO TFTs (a) annealed at 300, 400, and 500 °C and (b) with various mole ratios.

500 °C in Figure 6a and Table 1 showed a respective mobility of 7.99 and 9.82 $cm^2/(V\ s)$, an on-to-off current ratio of 1.93×10^6 and 3.68×10^6, a threshold voltage of 4.91 and 2.16 V, and a subthreshold slope of 0.82 and 0.73 V/dec. Comparing to previous oxide TFTs prepared with EHD-jet, 3.7 $cm^2/(V\ s)$ for IZO TFT[8] and 1.3 $cm^2/(V\ s)$ for IGZO TFT,[9] our result shows much improved mobility with better needle configuration. Transistor characteristics were also obtained for the EHD-jet ZTO TFTs at 300 °C, but the properties were inferior to the TFTs annealed at 400 and 500 °C, as shown in Figure 6a. The higher mobility of the TFTs at higher annealing temperatures was attributed to the modification of the semiconductor/interlayer interface, improved local atomic rearrangement, or decrease in the gap state and tail state near the conduction band minimum.[14] The observed negative shift in the threshold voltage was attributed to the higher intrinsic carrier concentrations for the films annealed at higher temperatures as well as to fewer lattice defects acting as electron traps.[21] Figure 6b and Table 2 showed the transfer characteristics of EHD-jet TFTS with precursors' mole ratios, resulting in better performance with 0.3 M. As the concentration of ZTO solution

Table 2. Electric Properties of EHD-Jet Printed ZTO TFTs at Concentrations of 0.1, 0.3, and 0.5 M

mole ratio	mobility ($cm^2 V^{-1} s^{-1}$)	on/off ratio	*V*th (V)	S−S (V dec^{-1})
0.1 M	4.72	7.88×10^5	8.32	0.98
0.3 M	9.82	3.68×10^6	2.16	0.73
0.5 M	5.99	1.81×10^6	−2.91	1.03

increases, the threshold voltage shifts negatively with channel thickness.[21] The optical images of ZTO patterns and their surface profiles are shown in Figure S2 in the Supporting Information. With low concentrations, the ZTO solution had widely spread on the substrate; however, with a higher concentrations, the pattern width decreased, resulting in a thicker film formation.

The hysteresis behavior was observed in the EHD-jet ZTO TFTs (Figure 7a). After a forward and backward bias, the hysteresis was 2.04 and 0.78 V at an annealing temperature of 400 and 500 °C, respectively. The presence of clockwise hysteresis in the transfer curves is consistent with electron

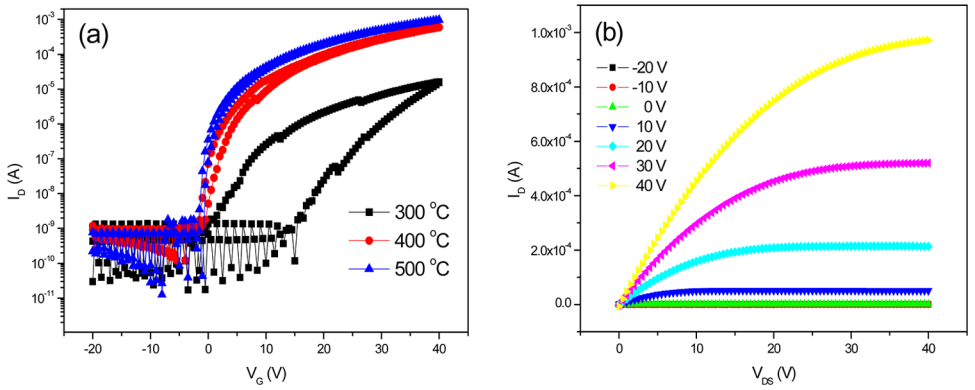

Figure 7. (a) Hysteresis characteristics and (b) output characteristics of the EHD-jet printed ZTO TFTs fabricated at various temperatures and at 500 °C, respectively.

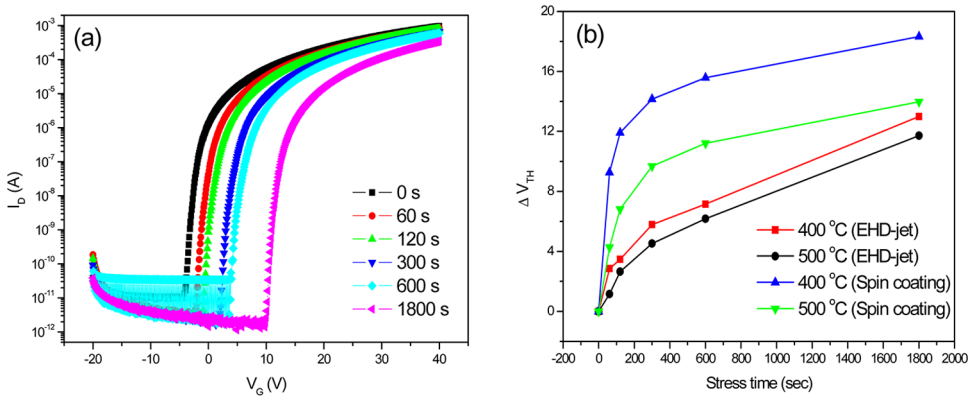

Figure 8. Transfer characteristics of (a) ZTO TFTs fabricated by EHD-jet annealed at (a) 500 °C under positive bias stress with gate voltage of 20 V and (b) threshold voltage shifts (Δ*V*th) of EHD-jet printed and spin-coated ZTO TFTs after positive bias stress for 1800 s.

trapping at or near the interface between the oxide semiconductor and the gate dielectric or within the oxide semiconductor channel layer.[22] The EHD-jet-printed ZTO TFTs showed good ohmic contact and solid output characteristics attributed to the fewer leakage current pathways, as shown in Figure 7b. Figure 8 shows the EHD-jet TFTs were subjected to gate-bias stress of *V*g = 20 V for 1800 s. The transfer curves measured from *V*g = −20 to 40 V with *V*d = 40 V. The shifts of the transfer curve of the EHD-jet ZTO TFT under bias stress increased with time. The threshold voltage *V*th shifts with the annealing temperatures of 400 and 500 °C were approximately 6 and 4 V, respectively, at an early stage of 300 s and increased slowly with time. In the case of the spin-coated ZTO TFTs, the positive bias stability showed an approximately 18 and 14 V shift at 400 and 500 °C, respectively. Significantly improved positive bias stability was obtained by EHD-jet processes compared to the spin-coated process as shown in Figure 8b. The positive *V*th shift with a positive bias voltage resulted from a negative charge either trapped at the interface between the channel and the dielectric or injected into the gate dielectric.[23] The increased electrical performance may be explained as follows. During EHD-jetting the solvent was partially vaporized due to the heated substrate and showed a similar effect to prebaking, which may facilitate better film formation, morphological texture formation, and better ZTO/SiO_2 interface formation. The root-mean-square roughness of the EHD-jet printed ZTO thin film was 0.325 nm, while that of the spin-coated one was 0.414 nm from the AFM measurement as shown in Figure S3 in the Supporting Information. Increased surface smoothness and decreased thickness of the channel positively affected the electrical properties. The patterned active layer obtained by EHD-jetting on a designated area also contributed to the improved properties.

CONCLUSIONS

ZTO TFTs were fabricated by an EHD-jet printing process. A ZTO active layer was patterned by optimization of the EHD-jet process parameters, and a 60 μm active layer width was obtained with a 100 μm metal nozzle. The electric properties of EHD-jet printed ZTO were superior to those of inkjet-printed and spin-coated ZTO TFTs. Transistor behaviors of EHD-jet ZTOs were obtained even at annealing temperatures of 300 °C. The electrical properties of EHD-jet printed ZTO TFTs showed a mobility of 9.82 $cm^2/(V\,s)$, an on−off current ratio of 3.7×10^6, a threshold voltage of 2.36 V, and a subthreshold slope of 0.73 V/dec at 500 °C. Much better hysteresis behavior and positive bias stability were also achieved using EHD-jet printing technology than spin-coated technology.

ASSOCIATED CONTENT

Supporting Information

This Supporting Information has O 1s XPS data, optical microscopic images with film morphology, and AFM images of the EHD-printed ZTO films. This material is available free of charge via the Internet at http://pubs.acs.org/.

AUTHOR INFORMATION

Corresponding Author

*E-Mail: wschoi@hoseo.edu. Phone: +82-41-540-5924.

Notes

The authors declare no competing financial interest.

ACKNOWLEDGMENTS

This work was supported by the Basic Science Research Program through the NRF funded by the Ministry of Education, Science and Technology (2012-039948).

REFERENCES

(1) Rajachidambaram, M. S.; Pandey, A.; Vilayurganapathy, S.; Nachimuthu, P.; Thevuthasan, S.; Herman, G. S. Improved Stability of Amorphous Zinc Tin Oxide Thin Film Transistors Using Molecular Passivation. *Appl. Phys. Lett.* **2013**, *103*, 171602.

(2) Lee, D.-H.; Han, S.-Y.; Hermane, G. S.; Chang, C.-H. Inkjet Printed High-Mobility Indium Zinc Tin Oxide Thin Film Transistors. *J. Mater. Chem.* **2009**, *19*, 3135−3137.

(3) Choi, W. S. Preparation of Zinc-Tin-Oxide Thin Film by Using an Atomic Layer Deposition Methodology. *J. Korean Phys. Soc.* **2010**, *57*, 1472−1476.

(4) Sanal, K. C.; Majeesh, M.; Jayaraj, M. K. Growth of IGZO Thin Film and Fabrication of Transparent Thin Film Transistor by RF Magnetron Sputtering. *Proc. SPIE* **2013**, *8818*, 881814.

(5) Tsay, C.-Y.; Fan, K.-S.; Wang, Y.-W.; Chang, C.-J.; Tseng, Y.-K.; Lin, C.-K. Transparent Semiconductor Zinc Oxide Thin Films Deposited on Glass Substrates by Sol-Gel Process. *Ceram. Int.* **2010**, *36*, 1791−1795.

(6) Kim, D.; Jeong, Y.; Song, K.; Park, S.-K.; Cao, G.; Moon, J. Inkjet-Printed Zinc Tin Oxide Thin-Film Transistor. *Langmuir* **2009**, *25*, 11149−11154.

(7) Park, J.-U.; Hardy, M.; Kang, S. J.; Barton, K.; Adair, K.; Mukhopadhyay, D. K.; Lee, C. Y.; Strano, M. S.; Alleyne, A. G.; Georgiadis, J. G.; Ferreira, P. M.; Rogers, J. A. High-Resolution Electrohydrodynamic Jet Printing. *Nat. Mater.* **2007**, *6*, 782−789.

(8) Lee, S.; Kim, J.; Choi, J.; Park, H.; Ha, J. Patterned Oxide Semiconductor by Electrohydrodynamic Jet Printing for Transparent Thin Film Transistors. *Appl. Phys. Lett.* **2012**, *100*, 102108.

(9) Jeong, S.; Lee, J.; Lee, S.; Seo, Y.; Kim, S.; Park, J.-U.; Ryu, B.-H.; Yang, W.; Moon, J.; Choi, Y. Metal Salt-Derived In-Ga-Zn-O Semiconductors Incorporating Formamide as a Novel Co-Solvent for Producing Solution-Processed, Electrohydrodynamic-Jet Printed, High Performance Oxide Transistors. *J. Mater. Chem. C* **2013**, *1*, 4236−4243.

(10) Kwack, Y.-J.; Choi, W.-S. Electrohydrodynamic Jet Spraying Technique for Oxide Thin-Film Transistor. *IEEE Electron Device Lett.* **2013**, *34*, 78−80.

(11) Khan, S.; Doh, Y. H.; Khan, A.; Rahman, A.; Choi, K. H.; Kim, D. S. Direct Patterning and Electrospray Deposition through EHD for Fabrication of Printed Thin Film Transistors. *Curr. Appl. Phys.* **2011**, *11*, S271−S279.

(12) Liang, Y. N.; Lok, B. K.; Wang, L.; Feng, C.; Lu, A. C. W.; Mei, T.; Hu, X. Effect of the Morphology of Inkjet Printed Zinc Oxide (ZnO) on Thin Film Transistor Performance and Seeded ZnO Nanorod Growth. *Thin Solid Films* **2013**, *544*, 509−514.

(13) Kwak, D.; Lim, J. A.; Kang, B.; Lee, W. H.; Cho, K. Self-Organization of Inkjet-Printed Organic Semiconductor Films prepared in Inkjet-Etched Microwells. *Adv. Funct. Mater.* **2013**, *23*, 5224−5231.

(14) Seo, S.-J.; Choi, C. G.; Hwang, Y. H.; Bae, B.-S. High Performance Solution-Processed Amorphous Zinc Tin Oxide Thin Film Transistor. *J. Phys. D: Appl. Phys.* **2009**, *42*, 035106.

(15) Jain, V. K.; Kumar, P.; Kumar, M.; Jain, P.; Bhandari, D.; Vijay, Y. K. Study of Post Annealing Influence on Structural, Chemical and Electrical Properties of ZTO Thin Films. *J. Alloys Compd.* **2011**, *509*, 3541−3546.

(16) Jeong, Y.; Bae, C.; Kim, D.; Song, K.; Woo, K.; Shin, H.; Cao, G.; Moon, J. Bias-Stress-Stable Solution-Processed Oxide Thin Film Transistors. *ACS Appl. Mater. Interfaces* **2010**, *2*, 611−615.

(17) Lee, J. S.; Choi, W.-S. Inkjet-Processed Zinc-Tin-Oxide Thin-Film Transistor with a MoO_3 Interlayer and Its Stability. *J. Korean Phys. Soc.* **2012**, *61*, 769−772.

(18) Kim, Y.-H.; Kim, K.-H.; Oh, M. S.; Kim, H. J.; Han, J. I.; Han, M.-K.; Park, S. K. Ink-Jet-Printed Zinc-Tin-Oxide Thin-Film Transistors and Circuits with Rapid Thermal Annealing Process. *IEEE Electron Device Lett.* **2010**, *31*, 836−838.

(19) Lee, C. G.; Dodabalapur, A. Solution-Processed Zinc-Tin Oxide Thin-Film Transistors with Low Interfacial Trap Density and Improved Performance. *Appl. Phys. Lett.* **2010**, *96*, 243501.

(20) Avis, C.; Jang, J. A High Performance Inkjet Printed Zinc Tin Oxide Transparent Thin-Film Transistor Manufactured at the Maximum Process Temperature of 300 °C and Its Stability Test. *Electrochem. Solid-State Lett.* **2011**, *14*, J9−J11.

(21) Lee, J. S.; Kwack, Y.-J.; Choi, W.-S. Inkjet-Printed In_2O_3 Thin-Film Transistor Below 200 °C. *ACS Appl. Mater. Interfaces* **2013**, *5*, 11578−11583.

(22) Lee, J. S.; Kwack, Y.-J.; Choi, W.-S. Low-Temperature Solution-Processed Zinc-Tin-Oxide Thin-Film Transistor and Its Stability. *J. Korean Phys. Soc.* **2011**, *59*, 3055−3059.

(23) Matters, M.; Leeuw, D.; Herwig, P.; Brown, A. Bias-Stress Induced Instability of Organic Thin Film Transistors. *Synth. Met.* **1999**, *102*, 998−999.